Available online at www.sciencedirect.com
SCIENCE DIRECT®
Cement & Concrete Composites 28 (2006) 384–392
Cement & Concrete Composites
www.elsevier.com/locate/cemconcomp

GPR inspection of concrete bridges

Johannes Hugenschmidt *, Roman Mastrangelo

EMPA, Swiss Federal Laboratories for Materials Testing and Research, Ueberlandstrasse 129, 8600 Duebendorf, Switzerland

Available online 11 April 2006

Abstract

Ground-penetrating-radar (GPR) has become an important method for the non-destructive testing of concrete bridges. Although there are standards and guidelines available today, the quality of results does not only depend on the object inspected but also on the qualification and experience of the team carrying out the radar survey. This situation is unsatisfactory for engineers that have to decide whether a radar survey is suitable to solve their problem.

EMPA has been active in the field of non-destructive testing of concrete structures for more than ten years. During this time, procedures for efficient data acquisition, processing interpretation and reporting have been developed. In addition, a large number of concrete structures has been inspected for research and services.

In a research project completed in 2005, radar inspections using the EMPA approach were carried out on bridges designated for demolition. Results were laid open before the bridges were taken down. After the demolition radar results were verified with the help of the bridge parts. Thus, the accuracy and reliability of radar surveys was quantified under realistic circumstances.

Keywords: Concrete bridges; Non-destructive-testing; Ground-penetrating-radar

1. Introduction

Ground-penetrating-radar (GPR) has become a valuable tool for the non-destructive testing of concrete bridges. Today there are standards [1] and guidelines [2] available. However, the choice of equipment, the setup of acquisition parameters and particularly the interpretation of radar data are within the responsibility of the team carrying out the radar survey and have a crucial influence on the quality of the results. Unfortunately, an assessment of this quality under realistic circumstances is in most cases impossible or restricted to few points. Laboratory experiments [3] provide information on the accuracy of inspections carried out under controlled conditions but their value is limited for estimating the quality of results under real field conditions.

This situation is unsatisfactory for engineers that have to decide whether a radar survey is suitable to solve their problem. In order to evaluate the accuracy and reliability of radar results on bridge decks under realistic circumstances, EMPA has carried out a research project sponsored by the Swiss Federal Roads Authority. Radar inspections were carried out on five bridges designated for demolition. Results were laid open before the bridges were taken down. During and after demolition radar results were verified with the help of the bridge parts where parameters such as the concrete cover of re-bar were measured manually with a ruler. In addition, a statistical analysis was carried out on radar data acquired during a survey aiming at the position of tendons in a bridge deck. This paper summarizes the results published in the research report [4] in March 2005.

2. Radar principles

Ground-penetrating-radar is an electromagnetic investigation method. It is also known as surface penetrating radar or electromagnetic reflection method. Mostly it is used in reflection mode where a signal is emitted via an

* Corresponding author. Tel.: +41 44 823 4318; fax: +41 44 821 6244.
E-mail address: johannes.hugenschmidt@empa.ch (J. Hugenschmidt).

0958-9465/$ - see front matter © 2006 Elsevier Ltd. All rights reserved.
doi:10.1016/j.cemconcomp.2006.02.016

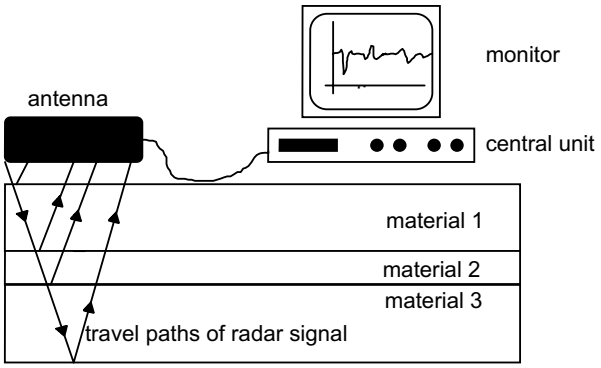

Fig. 1. Radar principles.

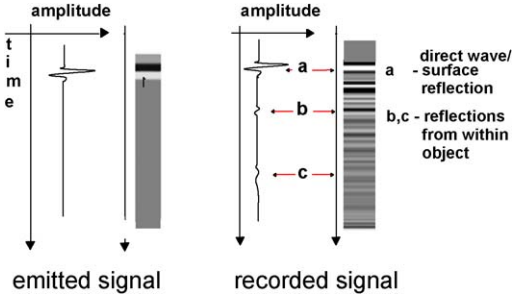

Fig. 2. Emitted and recorded signal.

antenna into the structure under investigation. Reflected energy caused by changes in material properties is recorded (Fig. 1) and analysed.

A sketch of the emitted and recorded signal in wiggle and grey scale mode is presented in Fig. 2. The signal recorded is usually referred to as a scan or a trace. The vertical axis is a time axis, its length in non-destructive-testing of concrete bridges is typically less than 30 nanoseconds (ns). In order to obtain depths the signal velocities in the different materials under investigation have to be known. There are several different ways to obtain these velocities. In the examples presented below signal velocities were defined by a comparison between radar data and borehole information.

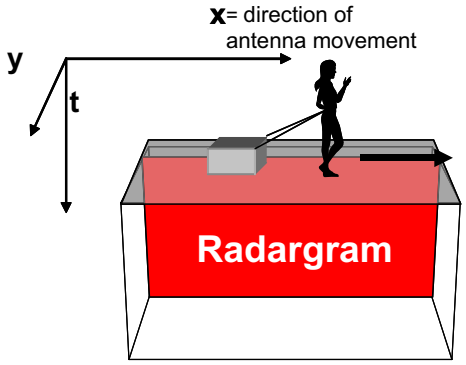

Fig. 3. Schematic sketch of a radargram.

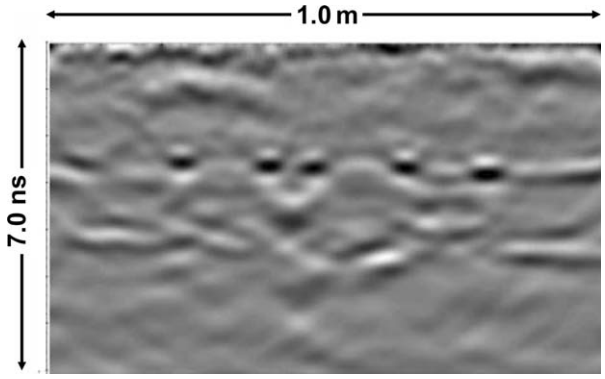

Fig. 4. Example of a radargram from concrete floor.

Radar data can be displayed in different ways. In all the examples shown below data are displayed in grey scale mode with two different configurations, as radargrams and as time slices. Radargrams consist of a large number of traces lined up according to their acquisition position as sketched in Fig. 3 where the antenna is moved in the x-direction recording data continuously. The radargram presented in Fig. 4 represents a dataset acquired along a line in the x-direction. The horizontal axis corresponds to the length in the x-direction and the vertical axis is a time axis.

When data are acquired not only along single lines but covering a whole area, for example by measuring along

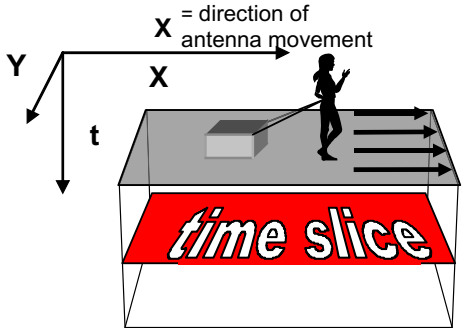

Fig. 5. Schematic sketch of a time slice.

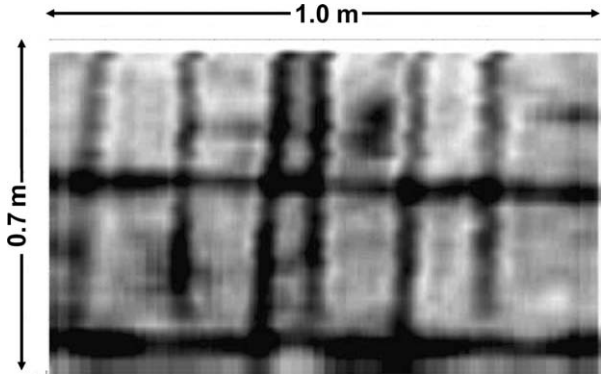

Fig. 6. Example of time slice from concrete floor.

many parallel lines, slices from different times/depths can be plotted (Fig. 5). The time slice presented in Fig. 6 corresponds to the data acquired on a surface along several parallel lines. Only signals recorded during a defined time-window are shown. Thus the two axis correspond to the surface on which data were acquired. Daniels [5] gives a detailed description of the concepts of Ground Penetrating Radar and its application on various problems from different fields of work.

3. Data acquisition

Obviously, when inspecting bridge decks or other large structures, the use of a mobile acquisition system is advantageous because of the reduction of acquisition time and the reduced obstruction to traffic flow. In Fig. 7, EMPA's mobile acquisition system is presented. It consists of a GSSI SIR-20 system, GSSI model 4205 horn antennas and additional equipment such as a survey wheel or additional antennas that can be mounted if required. A Trimble model 5700 RTK system is used for controlling the position.

Fig. 7. EMPA's mobile acquisition system for pavements and bridge decks.

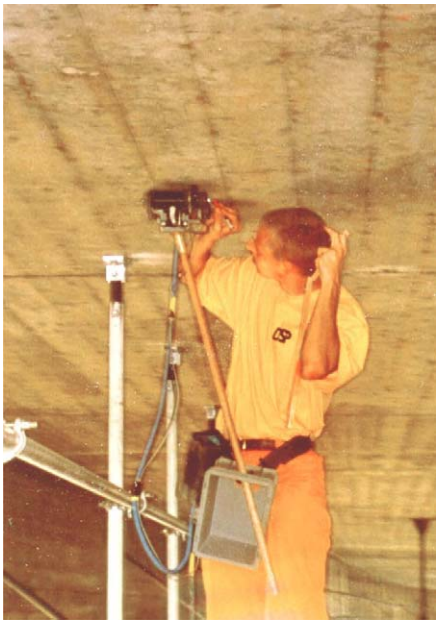

Fig. 8. Manual data acquisition on bottom side of bridge deck.

If the use of the mobile acquisition system is not possible, data have to be acquired manually. In Fig. 8, a GSSI model 5100 antenna is moved manually over the bottom side of a bridge deck for the detection of tendon ducts.

An overview of setups used for the examples presented in this paper is shown in Table 1. The centre frequencies listed are the result of investigations at EMPA. Two antennas (transmitter, receiver) of the same type were placed opposite to each other in air. The signal recorded with the receiver antenna was Fourier transformed and stacked in order to obtain the frequency range and centre frequency [6].

4. Processing

Data processing is an essential step within a radar survey. The optimal processing sequence depends on the radar

Table 1
Acquisition parameters for examples presented

No.	Application	Acquisition mode	Antenna type; centre frequency	Traces/meter; samples/trace	Data processing during data acquisition
1	Wyssenried bridge	Mobile, 10 km/h	GSSI Model 4205 horn; 1.2 GHz	200; 512	None
2	Ramp Sihl flyover	Mobile, 10 km/h	GSSI Model 4205 horn; 1.2 GHz	40; 512	None
3	Bridge deck, tendons	Manual	GSSI Model 5100; 1.2 GHz	300; 512	Bandpass filter, Gain
4	3-D survey on concrete girder	Manual	GSSI Model 5100; 1.2 GHz	400-spacing between acquisition lines 0.02 m; 512	None

data, the object under inspection and the problem to be solved by the radar survey. Some common aims of data processing are:

- Improvement of signal/noise ratio.
- Correction of surface reflection to time/depth zero.
- Migration (correction of the position of reflection energy that has been reflected sideways).
- Gain correction (amplification of signals depending on traveltime).

An example of a simple processing sequence applied to data acquired on an industrial railway track embedded in concrete is presented in Figs. 9–14. The length of the section shown is 3.0 m, the vertical time scale is 12 ns. The

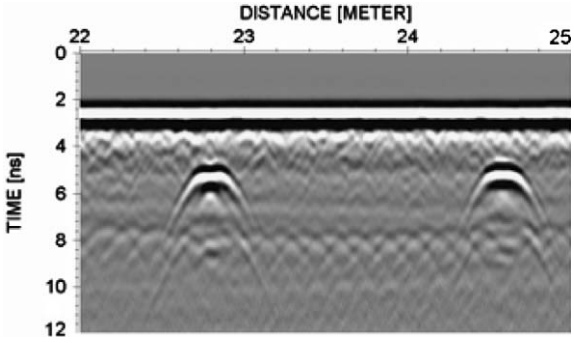

Fig. 9. Raw data before processing.

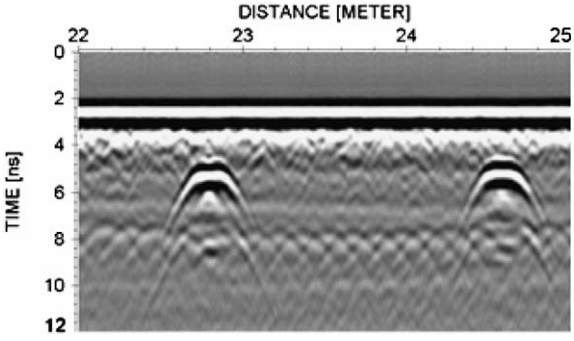

Fig. 10. Data after bandpass filtering.

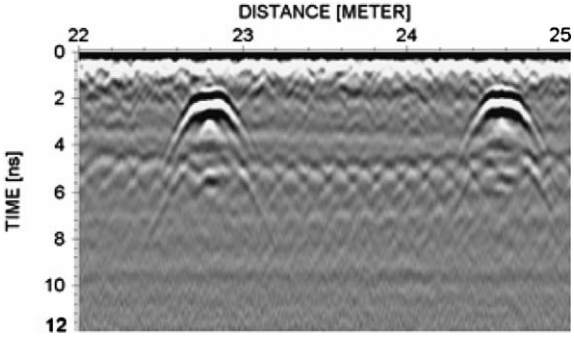

Fig. 11. Dataset after correction of surface reflection to time zero.

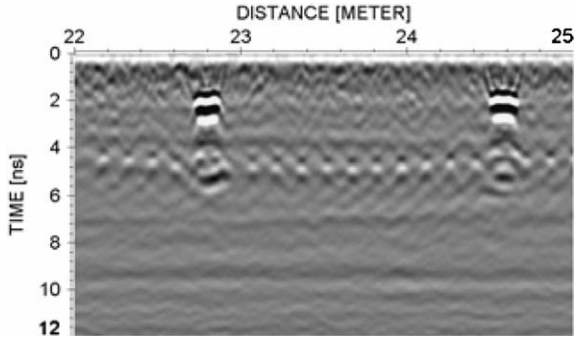

Fig. 12. Dataset after migration.

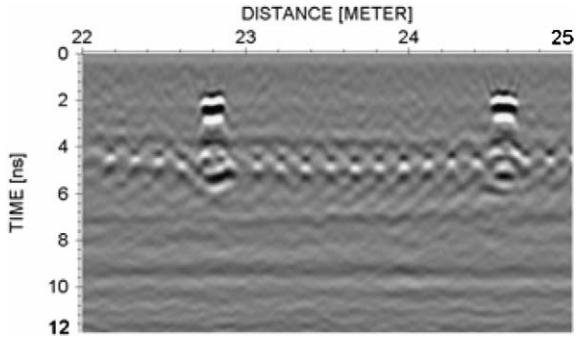

Fig. 13. Dataset after gain correction.

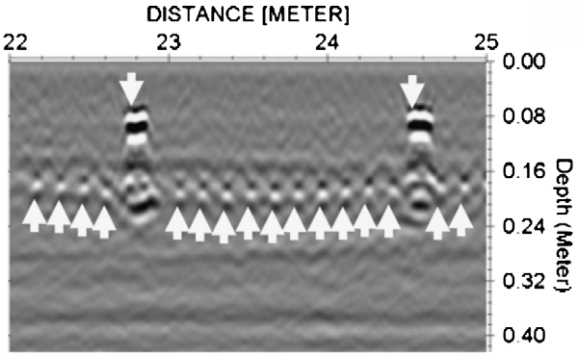

Fig. 14. Processed dataset with interpretation.

application of a bandpass filter (Fig. 10) results in this example only in a minor improvement of the signal/noise ratio. The correction of the surface reflection to time zero (Fig. 11) introduces the surface of the object under inspection as a reference plane for future depth calculations. It is also a necessary step before applying migration (Fig. 12), a processing step correcting the position of energy that has been reflected sideways. Migration is also referred to as synthetic aperture focussing technique (SAFT). Gain correction (Fig. 13) results in an amplification of energy reflected at greater depth.

In general it can be stated that the processing of radar data has many similarities to the processing of seismic and ultrasonic data. A comprehensive description of the

techniques used in seismic data processing can be found in Yilmaz [7].

5. Interpretation

During interpretation, reflections within radar data are related to physical structures within the object under inspection. Additional information such as building plans or borehole information is often necessary and always desirable to support the interpretation of radar data. In Fig. 14 the original time scale has been transformed into a depth scale using an estimated signal velocity within concrete of 0.08 m/ns. The two reflections at around 0.1 m were interpreted as sleepers and marked with arrows pointing downwards. The numerous reflections between 0.18 m and 0.20 m were interpreted as single bars of a layer of re-bar and marked with arrows pointing upwards.

6. Accuracy and reliability of results

In Fig. 15 a small bridge (Wyssenried bridge) is shown that had become redundant. Data acquisition was performed with EMPA's mobile GPR-unit. The acquisition parameters are listed in Table 1 (No. 1). A dataset after processing is shown in Fig. 16. The horizontal axis is 25 m long and corresponds to the length of the bridge,

Fig. 15. Wyssenried bridge.

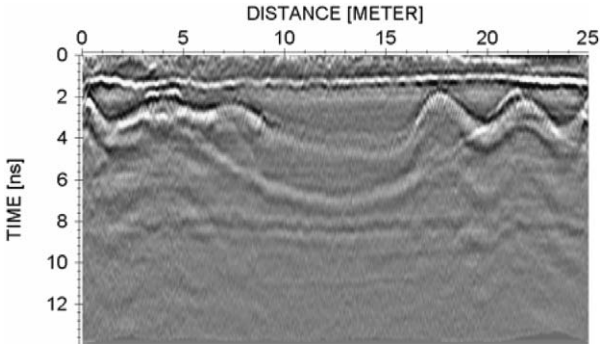

Fig. 16. Dataset from Wyssenried bridge.

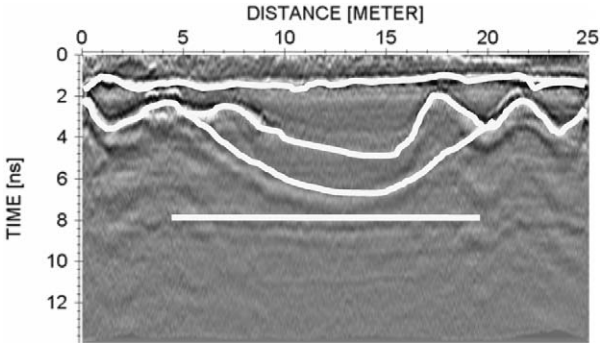

Fig. 17. Dataset with interpretation.

the vertical axis has a length of 14 ns. The interpretation of the radar data and the calibration of the time to depth/thickness conversion were supported by one borehole. A schematic view of the interpretation of the reflections marked with white lines is shown in Fig. 17. From top to bottom the reflections were interpreted as:

- Asphalt concrete interface.
- Top layer of re-bar.
- Tendon duct.
- Bottom of concrete slab.

The radar result for the concrete cover of re-bar using a constant signal velocity within concrete of $v = 0.082$ m/ns is presented in Fig. 18 (dashed line). Note that there are two gaps in the radar result, one at 4.0 m and one at 21.0 m due to the fact that the reflections from the top layer of re-bar and the tendon duct are overlapping in these areas. After the bridge deck had been sawed (Fig. 19), the concrete cover was measured manually with a ruler in distances of 1.0 m along the cut. The results of these manual measurements will be referred to as "reality" within this paper. The comparison between the results obtained by the radar survey (dashed line) and reality (solid line) is presented in Fig. 20 together with the absolute differences (solid circles) between those two results. The general course of the concrete cover over the length of the bridge is

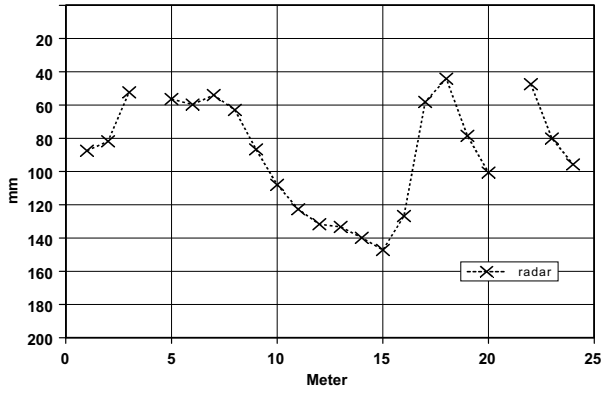

Fig. 18. Radar result for concrete cover of top layer of re-bar.

Fig. 19. Sawed bridge deck.

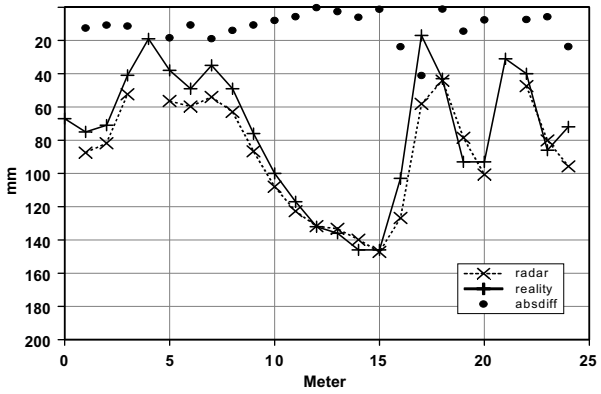

Fig. 20. Comparison between radar result and reality for concrete cover of re-bar.

mapped quite appropriately; the mean difference between the radar results and reality is 12 mm. However, it has to be mentioned that the maximum difference is 41 mm at 17.0 m.

Work on the other bridges has been carried out in accordance with the approach described above leading to an estimate for radar results for the concrete cover of the top layer of re-bar. The mean difference between radar and reality for all bridges was 10 mm, ranging between 3 mm and 17 mm for single objects. A result for the concrete cover was obtained on 77% of the sections inspected. No result was obtained on 23% of the sections inspected. This is mainly due to zones with a small concrete cover of re-bar leading to an overlap of the reflections at the top layer of re-bar and the asphalt-concrete interface, interpretation uncertainty in complex environments (for example when reflections from tendons or other structures can not be clearly distinguished from rebar reflections) and on and near joints.

In addition, the signal velocities minimizing the absolute differences between radar and reality were computed for all objects. Those velocities which can be expected to be close to the true signal velocities are ranging from 0.058 to 0.104 m/ns.

Fig. 21. Pavement removal with milling machine.

On none of the five bridges included in the project, information on deeper layers of re-bar was obtained when using the mobile acquisition unit.

The thickness of the asphalt pavement on concrete bridge decks is an important information for the planning of rehabilitation work and was therefore also included in this research project. On two of the bridges the pavement was removed with a milling machine (Fig. 21) and in one case the pavement was opened along lines with an excavator (Fig. 22) before the bridge deck was sawed. On two of the bridges a verification of the radar results for the pavement was not possible because the pavement had been removed before the radar survey or because it was destroyed with an excavator in an uncontrolled manner. The ramp of Sihl flyover (Fig. 23) was a temporary structure that had been built to enable access during major rehabilitation work on the main structure and the ramps. Radar data on this structure were acquired with the mobile unit using the acquisition parameters listed in Table 1 (No. 2). A dataset after processing is shown in Fig. 24. The horizontal axis is 40 m

Fig. 22. Pavement opening with excavator.

Fig. 23. Ramp of Sihl flyover.

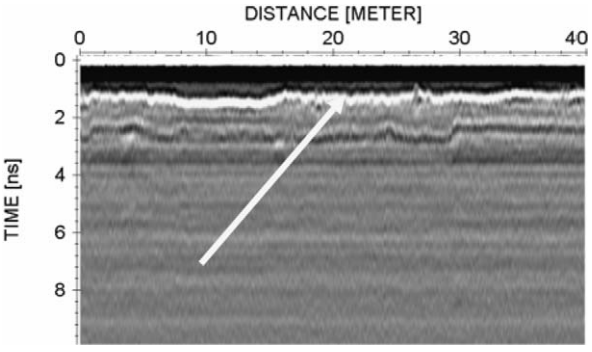

Fig. 24. Dataset from Sihl flyover ramp.

long. The reflection interpreted as resulting from the pavement–concrete interface is marked with a white arrow. The radar result for the pavement thickness using a constant signal velocity of $v = 0.143$ m/ns is shown in Fig. 25. The comparison between radar result (dashed line) and reality (solid line) together with the absolute differences (solid circles) is presented in Fig. 26. The mean difference between radar and reality for the three bridges was 9 mm, ranging between 5 mm and 11 mm for single objects. A result for

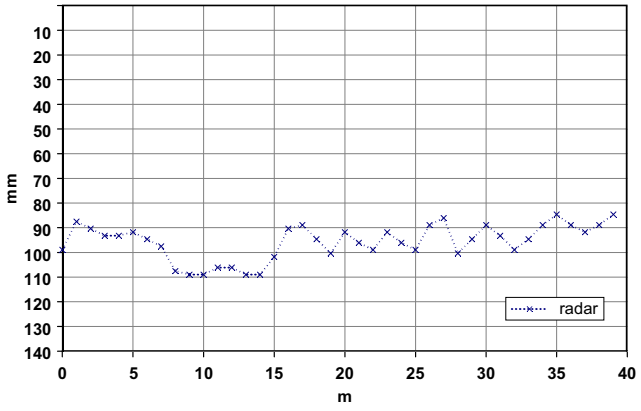

Fig. 25. Radar result for thickness of asphalt pavement.

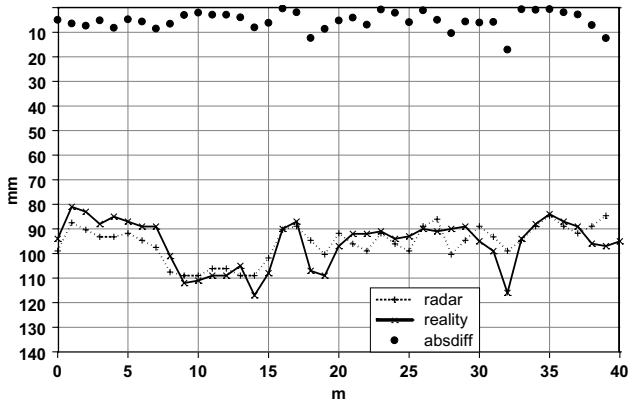

Fig. 26. Comparison between radar result and reality for thickness of asphalt pavement.

the thickness of the asphalt pavement was obtained on 95% of the sections inspected.

In addition, the signal velocities minimizing the absolute differences between radar and reality were computed for all objects. Those velocities which can be expected to be close to the true signal velocities are ranging from 0.117 and 0.143 m/ns.

A radar survey was carried on the bottom side of a concrete bridge deck (Fig. 8) to localize the position of tendons. Acquisition parameters are listed in Table 1 (No. 3). The length of the bridge was 1500 m and it had been put into service in 1974. The radar survey was carried out because the knowledge of the tendon positions was necessary for carrying out major rehabilitation work. Data interpretation was carried out on site in real time placing marks directly onto the concrete surface. As tendons were running orthogonal to the bridge axis, two lines parallel to the bridge axis were inspected. In order to evaluate the accuracy of the radar results a statistical test was carried out on nine sections with a total length of 105 m. A comparison of tendon positions between the two parallel lines led to a mean difference of 0.05 m.

In Fig. 27 two sections, each 5.0 m long from parallel lines are presented. Tendon positions are marked with vertical arrows. Please note that those positions are identical to those marked in real time onto the concrete. Obviously the distance between tendons is varying and not constant as indicated in the building plans. One tendon was missed in the upper section.

7. 3D-surveys

3-D surveys on concrete structures have the potential to reveal a detailed picture from the interior of concrete structures. In order to demonstrate this, a 3-D laboratory survey was carried out on a concrete girder (Fig. 28) of a bridge that had been demolished. Data were acquired manually with parameters listed in Table 1 (No. 4) both along horizontal and vertical lines on the area marked in Fig. 28. The

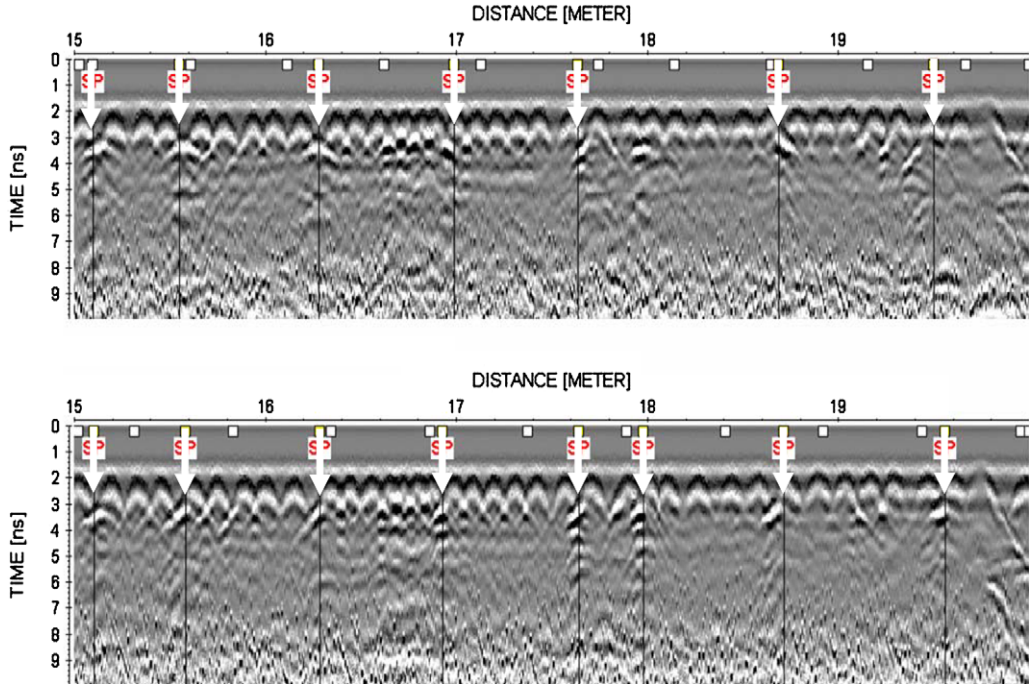

Fig. 27. Two radargrams acquired on parallel lines.

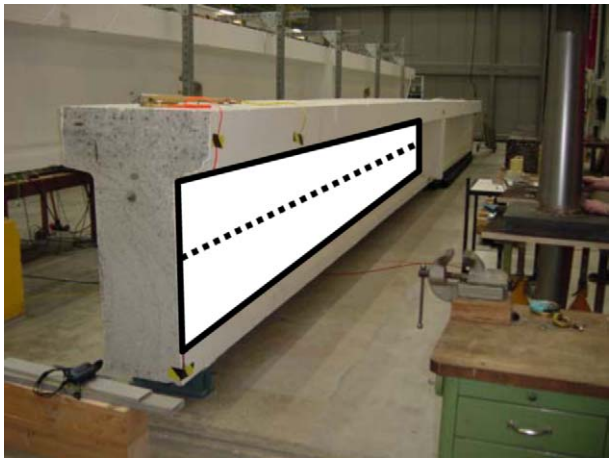

Fig. 28. Bridge girder with marked acquisition area.

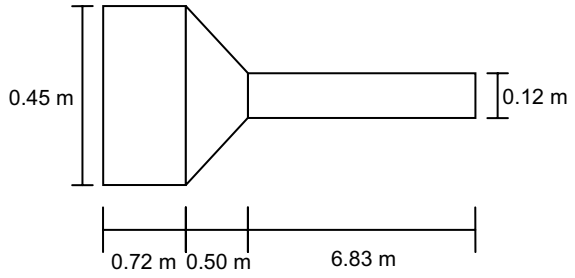

Fig. 29. Cross section of bridge girder (not to scale).

cross section of the girder along the dotted line in Fig. 28 is presented in Fig. 29.

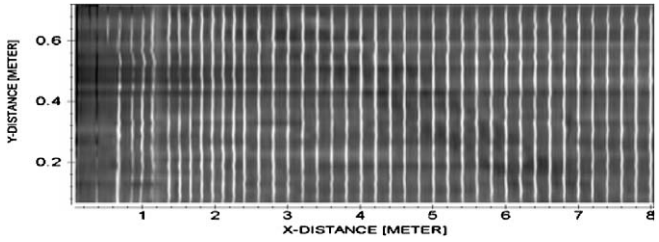

Fig. 30. Time slice from 0.51 ns, depth approximately 0.02 m.

Data acquired in longitudinal and vertical direction were processed separately with a two-dimensional processing sequence. Fig. 30 presents a time slice from the longitudinal dataset at 0.51ns corresponding to a depth of about 0.02 m. The dimensions of area shown in this and the following time slices are 8.05 m in the horizontal and 0.66 m in the vertical direction. Reflections from re-bars orthogonal to the direction of data acquisition are clearly visible. The time slice shown in Fig. 31 is from 1.13 ns corresponding to a depth of about 0.05 m. In addition to the reflection from the two tendon ducts running from top left to bottom

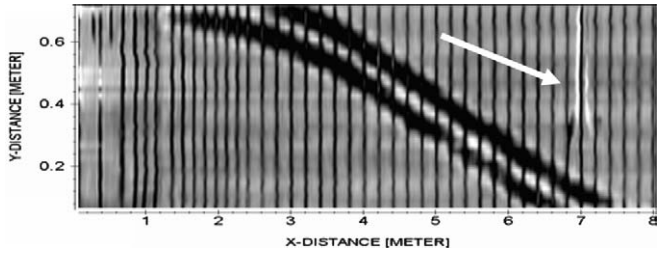

Fig. 31. Time slice from 1.13 ns, depth approximately 0.05 m.

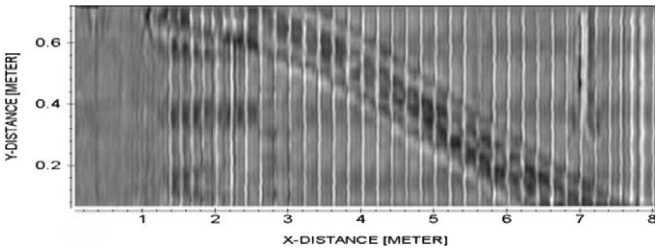

Fig. 32. Time slice from 2.15 ns, depth approximately 0.1 m.

right an additional nearly vertical reflection of unknown origin (white arrow in Fig. 31) can be spotted. The time slice presented in Fig. 32 from 2.15 ns corresponds to a depth of about 0.1 m. At this depth the reflection from the second layer of re-bars can be seen between 1.4 m and 8.0 m. Please note that the bars in Fig. 32 appear to be less focussed than those in Fig. 30 due to the damping of the high frequencies of the signal. Also, there are no bars visible between 0.0 m and 1.4 m because the girder is thicker there as can bee seen in Fig. 29.

3-D data can provide a detailed insight into concrete structures. However, the acquisition of 3-D datasets is time consuming when using a single antenna. Antenna arrays [8] or automatic scanner systems [9] can make the acquisition of 3-D data easier and thus encourage a wider use of 3-D techniques.

8. Conclusions

The concrete cover of the top layer of re-bar was determined on 77% of the inspected sections. The mean difference between radar results and reality was 10 mm. In addition, the spacing between single bars was determined in many places. Gaps in the result for the concrete cover were mainly the result of resolution problems in sections with a small cover and of interpretation uncertainties in areas with additional structural complexity.

No information about deeper layers of re-bar was obtained when the mobile acquisition unit was used.

The pavement thickness was determined on 95% of the inspected sections. The mean difference between radar results and reality was 9 mm. Gaps in the result for the pavement thickness were mainly due to a too small concrete cover resulting in overlapping reflections from bottom of pavement and re-bar.

In addition to the signal velocities obtained with the help of the boreholes which were used for the computation of pavement thickness and concrete cover of re-bar, signal velocities minimizing the absolute difference between radar results and reality were calculated. These velocities were varying between 0.058 m/ns and 0.104 m/ns for concrete and 0.117 m/ns and 0.143 m/ns for asphalt.

The positions of tendon-ducts in a bridge deck were determined with errors of less than 50 mm. The percentage of ducts that can be localized depends on the amount of effort and on the object under inspection.

3-D inspections provide a detailed insight into concrete structures. The use of antenna arrays or automatic scanner systems can encourage the wider use of 3-D techniques.

Acknowledgements

The project "Assessment of the condition of bridges with GPR" was sponsored by the Swiss Federal Roads Authority.

References

[1] Standard guide for using the surface ground penetrating radar method for subsurface investigation, Annual book of ASTM standards 2005, section four, Construction, vol. 04.09, soil and rock (II), D5714, designation: D 6432-99.
[2] Merkblatt über das Radarverfahren zur Zerstörungsfreien Prüfung im Bauwesen (instruction leaflet about the radar method for non-destructive-testing in civil engineering), German society for non-destructive-testing, November 2001 [in German].
[3] Watanabe S, Misra S, Oumoto T. Nondestructive evaluation of concrete structures. In: Proc non-destructive testing in civil engineering 2003, 16–19 September, 2003, Berlin, D.
[4] Hugenschmidt J. Zuverlässigkeit und Genauigkeit von Georadar-Ergebnissen auf Brücken (Reliability and Accuracy of radar results on concrete Bridges). Federal Department of Environment, Transport, Energy and Communications, Swiss Federal Roads Authority, Report No. 582, March 2005 [in German].
[5] Daniels D. Ground penetrating radar. 2nd ed. The Institution of Electrical Engineers; 2004.
[6] Hugenschmidt J. Multi-offset-analysis for man-made structures, GPR 2000. In: 8th international conference on ground penetrating radar, 23–26 May, 2000, Gold Coast, Australia.
[7] Yilmaz O. Seismic data processing. Society of Exploration Geophysicists; 1987.
[8] Eide E, Hjelmstad J. 3D utility mapping using electronically scanned antenna array. In: Proc 9th international conference on ground penetrating radar. Santa Barbara, USA, April 29–May 2, 2002.
[9] Taffe A, Borchhardt K, Wiggenhauser H. Specimen for the improvement of NDT-methods, design and construction of a large concrete slab for NDT methods at BAM. In: Proc NDT-CE 2003, 16–19 September, Berlin/Germany.